

# ANALYSIS OF PARTIAL DISCHARGE SIGNALS WITH HIGHER DIMENSION CHROMATICITY

A. A. AL-TEMEEMY<sup>1</sup>, G. R. JONES<sup>2</sup>, M. RAGAA<sup>3</sup>, C. NYAMUPANGEDENGU<sup>4</sup>,  
A. G. DEAKIN<sup>2\*</sup> AND J. W. SPENCER<sup>2</sup>

<sup>1</sup> Laser and Optoelectronics Engineering Department, Al Nahrain University, Baghdad, Iraq

<sup>2</sup> Centre for Intelligent Monitoring Systems, Department of Electrical Engineering and Electronics, University of Liverpool, L69 3GJ, UK

<sup>3</sup> Northern Powergrid, 98 Aketon Road, Castleford, WF10 5DS, UK

<sup>4</sup> School of Electrical and Information Engineering, University of the Witwatersrand, Johannesburg, SA

\*[anthonyd@liv.ac.uk](mailto:anthonyd@liv.ac.uk)

## ABSTRACT

An extension of the chromatic approach [1] for analysing Partial Discharge (PD) signals is described. This involves a different pre-processing approach and the use of extended chromatic maps based upon the signal amplitude as well as phase angle domain. Examples are presented of this approach for quantifying additional features of real PD signals to discriminate between different PD conditions.

## 1. INTRODUCTION

Monitoring Partial Discharges (PD) remains a means for assessing the electrical insulation integrity of high voltage equipment. This requires quantification for discriminating PD signals. In addition to conventional signal processing techniques such as neural networks, expert systems, fuzzy logic etc. [2], [3], a novel means of PD signal quantification based upon chromatic techniques has been demonstrated [1]. It has been shown how such an approach can track PD development with time and voltage prior to full electrical breakdown. The potential of the chromatic approach has been shown for discriminating between different types of PD, for quantifying the degree of symmetry of the Partial Discharge activity and for indicating the effect of alternating voltage polarity etc.

This contribution shows how the chromatic approach can be extended to provide more detailed PD discrimination. This involves the use

of three chromatic processors along the signal amplitude domain in addition to the three processors along the phase angle domain. A new form of Chromatic map is described for quantifying additional signal features.

## 2. PD SIGNAL PROCESSING

### 2.1 Chromatic procedures

The present chromatic analysis approach addresses the PD amplitude – phase signal in two domains rather than a single, Phase Angle domain as in [1]. The signal is converted from its one dimensional vector form of magnitude in pC ( $v$ ) as a function of phase angle ( $h$ ) (i.e.  $v(h)$ ) into a two dimensional vector form,  $S(v, h)$  where  $S(v, h) = 1$  if a signal exists at  $(v, h)$ , 0 otherwise. Chromatic processing involves addressing the PD signal with two sets of three processors (R, G, B) one set for each of the two domains. In each domain the three processors have overlapping responses. The output of each processor is of the form [4] represented by (1),

$$Q(M)_o = \sum_h \sum_v Q(M)_{RS(v, h)} \quad (1)$$

where  $Q(M)R$  represents the responses  $R(M)$ ,  $G(M)$  or  $B(M)$ ,  $M \rightarrow h, v$  for the processors along the phase angle and amplitude axes respectively (Figs. 1 (a) and (b)). These outputs are normalised with respect to the area under the response curve for each processor according to

$$(2), \quad Q(M)_n = [Q(M)_o \cdot sf] / [vl \cdot hl] \quad (2)$$

where  $hl$  = phase angle range ( $90^\circ$  for the present conditions),  $vl$  = maximum amplitude,  $sf$  =

sampling factor range. Chromatic parameters may then be derived as [4]:

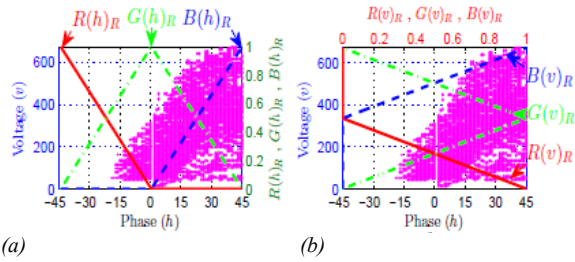


Fig. 1 Non-Orthogonal Chromatic Processors  
(a) Processors along phase angle axis (h)  
(b) Processors along signal amplitude axis (v)

$$L(M) = [R(M)n + G(M)n + B(M)n] / 3 \quad (3)$$

$$X(M) = R(M)n / 3L(M) \quad (4a)$$

$$Y(M) = G(M)n / 3L(M) \quad (4b)$$

$$Z(M) = B(M)n / 3L(M) \quad (4c)$$

where  $M = h$  (phase) or  $v$  (amplitude) domains. A PD signal may then be represented on various chromatic maps –

$L(h):y(h)/z(h) \rightarrow$  signal strength:dominant value

$y(h):z(h) \rightarrow$  dominant value and signal spread [1]

$y(v):z(v) \rightarrow$  signal shape (kurtosis, Fig. 2(b)).

A combined  $y(h):z(h)$  and  $y(v):z(v)$  map is shown on Fig. 2(a) and an illustration of signal shapes of different kurtosis shown on Fig. 2(b). This means that a PD signal may be quantified by five parameters –  $L(h)$ ,  $y(h)$ ,  $z(h)$ ,  $y(v)$ ,  $z(v)$ . (Note that on the  $y(v):z(v)$  map  $y(v) < \sim z(v)$  is indicative of two clusters of points separated by a large gap).

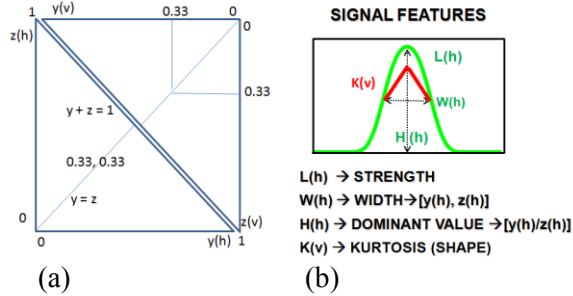


Fig. 2  $y(h):z(h)$  and  $y(v):z(v)$  Chromatic Mapping  
(a) Combined  $y(h):z(h)$  and  $y(v):z(v)$  maps  
(b) Illustration of signal features

### 3. EXTENDED CHROMATIC MAPS

The deployment of the extended chromatic analysis may be illustrated with some simple signal envelopes expanding along the phase angle (h) and signal amplitude (v) dimensions. Fig. 3(a) shows examples of step (i), ramp (ii), and parallel gap (iii) signals expanding along the phase angle axis (h) and a parallel gap with the gap width varying (iv). Fig. 3(b) shows a L versus  $y(h) / z(h)$  map with each of the four

signals from Fig. 3(a). Figs. 3(c) (i), (ii), (iii), (iv) show respectively the extended chromatic maps ( $z(h) : y(h)$ ,  $z(v) : y(v)$ ) for the step, ramp, parallel band signals of Figs. 3(a). Figs. 3(c) (i), (ii), (iii) relate to each signal spreading along the phase angle axis, whilst Fig. 3(c) (iv) is for the gap between the parallel bands (Fig. 3 (a) (iv)) varying. The  $L : y(h)/z(h)$  map shows that the phase expanding step and ramp signals are distinguishable on such a map, but the expanding parallel gap signal is similar to the expanding step and therefore is not distinguishable. The parallel gap width results show changes in the L parameter but not  $y(h)/z(h)$ .

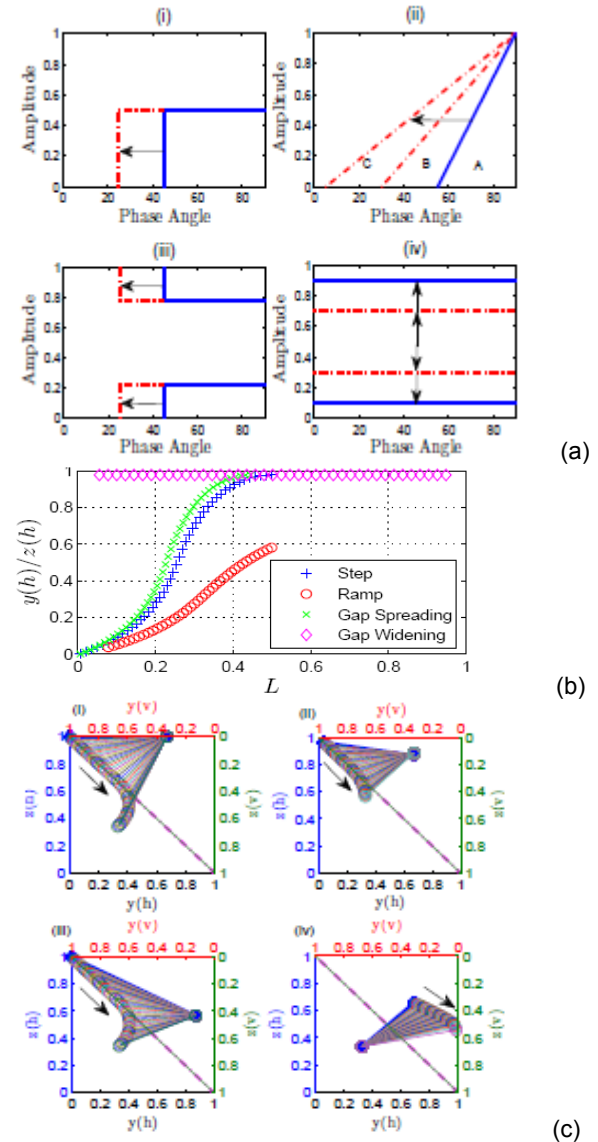


Fig. 3 2 - D Chromatic Transformation of some simple signals  
(a) Amplitude versus Phase Angle (0 – 90°) –  
(i) step (ii) ramp (iii) parallel gap – all spreading signal envelopes  
(iv) parallel gap – gap widening  
(b)  $y(h)/z(h)$  versus L map for step, ramp, parallel gap spreading and parallel gap widening  
(c) Combined  $y(h):z(h)$  and  $y(v):z(v)$  maps  
(i) step (ii) ramp (iii) parallel gap – all spreading signal envelopes  
(iv) parallel gap – gap widening

Figures 3(c) (i), (ii), (iii) show that the variation of  $z(h):y(h)$  with phase angle spread for each of the step, ramp and parallel gap signals lie along the locus  $z(h) + y(h) = 1$ , and so are not distinguishable on such a map. Because of the fixed amplitude of each signal during phase angle expansion, the  $z(v):y(v)$  coordinates of each signal remain invariable. The parallel bands signals are distinguished from the others by  $z(v) > y(v)$ . Figure 3(c) (iv) shows that as the gap width of the parallel bands increases,  $z(v)$  increases as  $y(v)$  decreases.

#### 4. APPLICATION TO PD SIGNALS

The extended chromatic mapping described in section 3 may be applied to real PD signals to

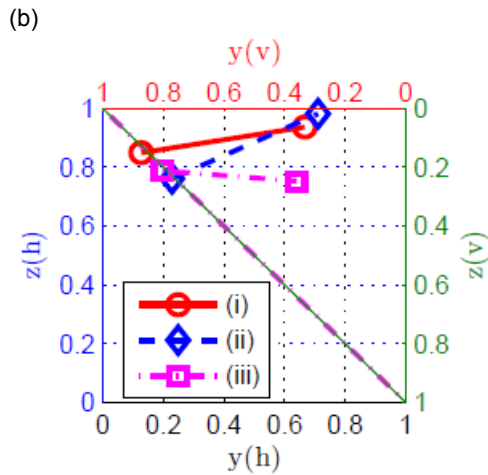
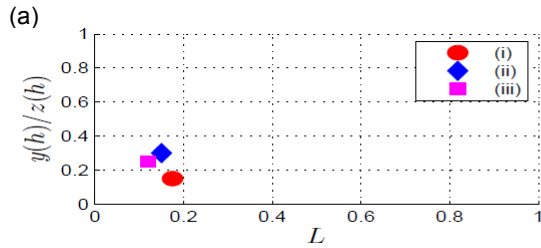
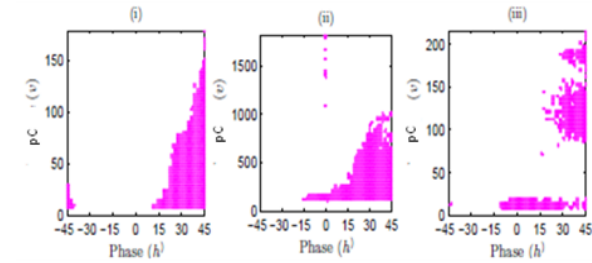


Fig. 4 Un-aged samples  
 (a) Raw signals ( $-45 \rightarrow +45^\circ$  phase angles)  
 (i) high amplitude, short spread (ii) low amplitude, long spread  
 (iii) clusters of PD activities  
 (b)  $L$  versus  $y(h)/z(h)$  map  
 (c) Combined  $y(h):z(h)$  and  $y(v):z(v)$  maps

yield additional signal discrimination to that provided by the  $z(h):y(h)$  mapping in [1].

#### 4.1 Un-aged Insulation

Fig. 4 (a) shows three PD signals for some un-aged XLPE insulated power cable samples [5] covering the phase angle range of  $-45 \rightarrow +45^\circ$  around the zero voltage crossing of an applied alternating voltage. Figs. 4(a) (i) (ii) (iii) show respectively a higher amplitude signal of short phase angle spread, a signal of a relatively low amplitude with extended phase angle spread, and a signal with clusters of PD activities separated by clear gaps. The signals were addressed with phase angle and amplitude processors, the latter covering the amplitude range of each signal (which differ from each other).

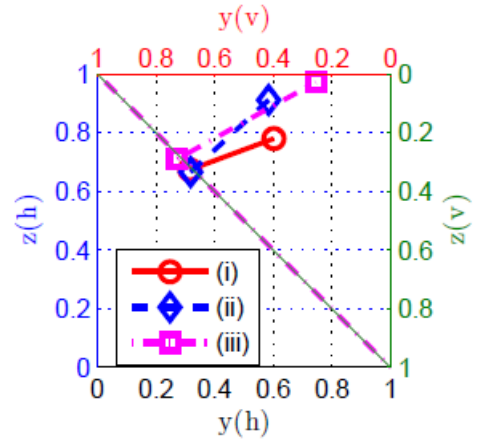
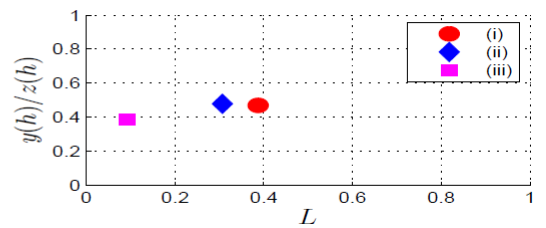
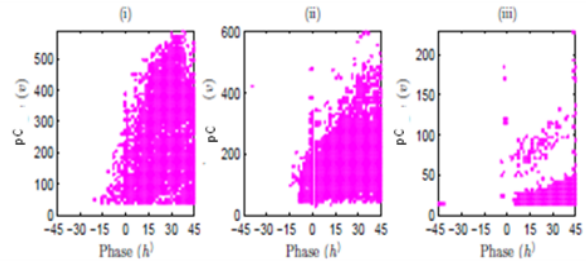


Fig. 5 Aged samples  
 (a) Raw signals ( $-45 \rightarrow +45^\circ$  phase angles)  
 (i) high amplitude, wide extent (ii) moderate amplitude, less well defined cluster (iii) low amplitude well formed clusters of PD activities  
 (b)  $L$  versus  $y(h)/z(h)$  map  
 (c) Combined  $y(h):z(h)$  and  $y(v):z(v)$  maps

Fig. 4(b) shows the L:(y(h)/z(h)) map coordinates of the three signals of Fig. 4(a) to be  $\sim 0.15-0.3$ . Fig. 4(c) shows the three signals represented on an extended chromatic map with all three signals lying on the  $z(h) + y(h) = 1$  locus. The y(v) coordinates of the three signals are similar (0.3, 0.33, 0.35), as are the z(v) coordinates of the single cluster signals (Fig. 4(a) (i),(ii)) ( $< 0.1$ ). However the z(v) coordinate of the double cluster signal is significantly higher (0.25) than the single cluster signals.

#### 4.2 Aged Insulation

Fig. 5(a) shows three PD signals (within the phase angle range  $-45 \rightarrow +45^\circ$ ) from power cable samples aged through exposure to repetitive lightning shaped voltage impulses [5]. Fig. 5(a) (i) shows a signal of substantial amplitude and phase spread ( $\sim 600\text{pC}$ ,  $+45 \rightarrow -15^\circ$ ). Fig. 5(a) (ii) shows a signal of similar amplitude and spread but with more peripheral fragments. Fig. 5(a) (iii) shows a signal of moderate amplitude ( $\sim 200\text{pC}$ ) consisting of two bands, the higher band less well defined than the lower one. Fig. 5(b) shows the L:(y(h)/z(h)) map coordinates of the three signals of Fig. 5(a) to be in the range 0.1-0.4, 0.4-0.5. Fig. 5(c) shows all three signals to have similar z(h), y(h) coordinates ( $\sim 0.7$ , 0.3) on the  $z(h) + y(h) = 1$  locus. The z(v), y(v) coordinates of (i), (ii), (iii) are respectively (0.22,0.39), (0.09,0.42), (0.03,0.26).

### 5. DISCUSSION OF RESULTS

The PD signals should first be assessed via the overall strength and extent of the PD activity using the L:(y(h)/z(h)) maps (Figs. 4(b), 5(b)). These show that the un-aged samples (Fig. 4(b)) have lower values of the spread parameter (y(h)/z(h)) than the aged samples and that two of the aged samples ((i), (ii)) have 1.5-2 times the L values of the un-aged samples. However the two cluster aged sample has a similar value to the un-aged samples. The higher PD activity quantified by these results may indicate more progression for the aged samples towards breakdown. The y(h):z(h) maps imply that because all samples (aged and un-aged) lie on the locus  $y(h) + z(h) = 1$ , immediate breakdown may not be imminent since y(h), z(h) are not close to 0.33, 0.33 [1]. However the three aged samples have progressed further along the locus (z(h)  $\sim 0.7$ ) than the un-aged samples (z(h)  $> 0.7$ ). The un-aged y(v):z(v) map (Fig. 4(c)) indicates that the two PD clusters

of Fig. 4(a) (iii) produce a higher value of z(v). The sample of Fig. 5(a) (i) has similar values to the single cluster of Fig. 4(a) (iii) in accordance with Fig. 3. However the two cluster signal (Fig. 4(a) (iii)) has a lower value of L. The weak cluster of Fig. 5(a) (iii) has lower values of z(v) and L, similar to the other samples of Figs. 4(a) (i), (ii), and 5(a) (ii).

### 6. CONCLUSIONS

It has been shown how the chromatic analysis of PD signals can be extended to provide further signal discrimination by using two sets of orthogonal processors one to address the amplitude domain and the other the phase angle domain. Preliminary results have been presented which show that the approach has the potential for distinguishing signal kurtosis. With further work the approach might also be extendable to identify more unambiguously two distinct signal clusters (e.g. Fig. 5(a) (iii) as well as Fig. 4(a) (iii)) which may be indicative of separate PD sources.

### REFERENCES

- [1] M. Ragaa, G. R. Jones, A. G. Deakin, J. W. Spencer, "Chromatic Mapping of Partial Discharge Signals", High Voltage Engineering ISSN 1003-6520, Vol. **39**, No. 10, pp. 2532 – 2540, 2013.
- [2] T. Abdel-Galil, R. M. Sharkawy, M. M. A. Salma, R. Bartnikas, "Partial Discharge Pulse Recognition using an Inductive Inference Algorithm", IEEE Trans. on Dielectrics and Electrical Insulation, **28**, 6, pp. 1016 - 1024, 2005.
- [3] Y. Tu, Z. D. Wang, P. A. Crossley, "Partial Discharge Pattern Recognition Based on 2-D Wavelet Transform and Neural Network Techniques", IEEE Power Engineering Society Summer Meeting, IEEE., Chicago, IL., USA, **1**, pp. 411 - 416, 2002.
- [4] G. R. Jones, A. G. Deakin, J. W. Spencer, *Chromatic Monitoring of Complex Conditions*, Taylor and Francis, Florida, USA, ISBN-13: 978-1-58488-988-5, 2008.
- [5] M. M. Mampane, "An investigation into partial discharge behaviour in impulse-aged polymer insulation", MSc. Dissertation, University of the Witwatersrand, Johannesburg, 2013.